HHS Public Access

Author manuscript

J Neurochem. Author manuscript; available in PMC 2017 September 01.

Published in final edited form as:

J Neurochem. 2016 September ; 138(6): 806–820. doi:10.1111/jnc.13718.

Functional interaction between Lypd6 and nicotinic acetylcholine receptors

Maria Arvaniti[1], **Majbrit M. Jensen**[2], **Neeraj Soni**[1], **Hong Wang**[3], **Anders B. Klein**[1], **Nathalie Thiriet**[4], **Lars H. Pinborg**[2,5], **Pretal P. Muldoon**[6], **Jacob Wienecke**[7], **M. Imad Damaj**[6], **Kristi A. Kohlmeier**[1], **Marjorie C. Gondré-Lewis**[3], **Jens D. Mikkelsen**[2], and **Morten S. Thomsen**[1,2,*]

[1]Department of Drug Design & Pharmacology, University of Copenhagen, Copenhagen Denmark

[2]Neurobiology Research Unit, University Hospital Copenhagen, Rigshospitalet, Copenhagen, Denmark

[3]Laboratory for Neurodevelopment, Department of Anatomy, Howard University College of Medicine, Washington D.C., USA

[4]Laboratory of Experimental and Clinical Neurosciences, University of Poitiers, Poitiers, France

[5]Epilepsy Clinic, University Hospital Copenhagen, Rigshospitalet, Copenhagen, Denmark

[6]Department of Pharmacology and Toxicology, Medical College of Virginia, Virginia Commonwealth University, Richmond, VA, USA

[7]Department of Nutrition, Exercise and Sport & Department of Neuroscience and Pharmacology, University of Copenhagen, Denmark

Abstract

Nicotinic acetylcholine receptors (nAChRs) affect multiple physiological functions in the brain and their functions are modulated by regulatory proteins of the Lynx family. Here, we report for the first time a direct interaction of the Lynx protein LY6/PLAUR domain-containing 6 (Lypd6) with nAChRs in human brain extracts, identifying Lypd6 as a novel regulator of nAChR function.

Using protein cross-linking and affinity purification from human temporal cortical extracts, we demonstrate that Lypd6 is a synaptically enriched membrane-bound protein that binds to multiple nAChR subtypes in the human brain. Additionally, soluble recombinant Lypd6 protein attenuates

[*]**Corresponding Author:** Morten Skøtt Thomsen, Ph.D., Department of Drug Design and Pharmacology, Faculty of Health and Medical Sciences, University of Copenhagen, Jagtvej 160, building 22, C.421, 2100 Copenhagen, Denmark, morten.s.thomsen@sund.ku.dk.

Involves human subjects: Yes

If yes: Informed consent & ethics approval achieved: Yes => if yes, please ensure that the info “Informed consent was achieved for all subjects, and the experiments were approved by the local ethics committee.” is included in the Methods.

ARRIVE guidelines have been followed:

Yes

=> if No, skip complete sentence

=> if Yes, insert “All experiments were conducted in compliance with the ARRIVE guidelines.”

Conflicts of interest: none

=> if ’none’, insert “The authors have no conflict of interest to declare.”

=> otherwise insert info unless it is already included

---

nicotine-induced hippocampal inward currents in rat brain slices and decreases nicotine-induced ERK phosphorylation in PC12 cells, suggesting that binding of Lypd6 is sufficient to inhibit nAChR-mediated intracellular signaling. We further show that perinatal nicotine exposure in rats (4mg/kg/day through minipumps to dams from embryonic day 7 to postnatal day 21) significantly increases Lypd6 protein levels in the hippocampus in adulthood, which did not occur after exposure to nicotine in adulthood only.

Our findings suggest that Lypd6 is a versatile inhibitor of cholinergic signaling in the brain, and that Lypd6 is dysregulated by nicotine exposure during early development.

Keywords

nicotine; Lynx; Ly-6; LY6/PLAUR domain-containing 6; affinity purification

Introduction

Members of the Ly-6/neurotoxin (Lynx) superfamily have been used for decades as lymphocyte differentiation markers (Bamezai 2004). More recent research has shown that several Lynx proteins are expressed in the brain (reviewed in (Julie M Miwa, Lester, and Walz 2012)). Lynx proteins are characterized by a three-dimensional consensus motif, termed the three-finger fold, that mediates protein-protein binding (Tsetlin 1999), and most Lynx proteins are attached on the cell membrane through a glycosylphosphatidylinositol (GPI) anchor (Adermann et al. 1999). The Lynx proteins Lynx1 and Lynx2 have been shown to form stable complexes with, and negatively modulate the response of, α7 and α4β2 nicotinic acetylcholine receptors (nAChRs) (Fu, Rekow, and Spindel 2012; Tekinay et al. 2009; Julie M Miwa et al. 2006). Furthermore, Lynx1 knock-out mice exhibit improved associative learning in a fear-conditioning paradigm (Miwa et al. 2006), and it was recently shown that Lynx1, acting through nAChRs, is critical for the loss of synaptic plasticity in the visual cortex that occurs in adulthood (Morishita et al. 2010). These results suggest that Lynx1 can bind to and modulate nAChR function in the brain, and that this has important consequences for synaptic plasticity and memory (reviewed in (Julie M Miwa, Freedman, and Lester 2011; Thomsen and Mikkelsen 2012; Julie M Miwa, Lester, and Walz 2012)). However, it is currently not known whether this regulation of the cholinergic system is unique to Lynx1 or whether it extends to other members of the Lynx family.

LY6/PLAUR domain containing 6 (Lypd6) is a Lynx protein that is expressed in the human and rodent nervous system (Darvas et al. 2009; Zhang et al. 2010). In the mouse visual cortex, Lypd6 and Lynx1 are mainly expressed in GABAergic interneurons, where they exhibit complementary expression patterns; the former is exclusively expressed in somatostatin and the latter is restricted in parvalbumin interneurons (Demars and Morishita 2014). This implies that Lypd6 may be involved in modulation of nAChRs in neuronal circuits distinct from Lynx1. Lypd6 is an important regulator of embryogenesis in zebrafish through its enhancement of Wnt/β-catenin signaling (Özhan et al. 2013), and Lypd6 knock-down in mice results in small litter size and lack of ability to procreate, suggesting impaired germ cell or embryonic development (Darvas et al. 2009). In humans, two distinct microduplications of the 2q23.1 chromosomal region containing the Lypd6 gene resulted in

severe intellectual disability and autistic features (Chung et al. 2012). Transgenic overexpression of Lypd6 in mice increases the Ca^{2+}-component of nicotine-induced currents in dissociated trigeminal ganglion neurons and results in behaviours indicative of an increased cholinergic tone, such as locomotor arousal, hypoalgesia, and pre-pulse inhibition of the acoustic startle response (Darvas et al. 2009). This invites the possibility that Lypd6, like Lynx1 and Lynx2, modulates nAChR function by binding to nAChRs. However, to our knowledge, there is no report of interactions of Lynx proteins with native nAChRs in the human brain.

Nicotine, the major pharmacologically active chemical found in tobacco smoke, is another important regulator of the cholinergic system through its modulation of nAChRs in animals and humans. Pre- or perinatal exposure to smoking or nicotine alone can produce long term alterations in several transmitter systems including the glutamatergic, serotonergic and dopaminergic (H Wang et al. 2011; Muneoka et al. 1997) and is associated with development of anxiety, attention deficit hyperactivity disorder, memory deficits, and other cognitive deficits (reviewed in (Blood-Siegfried and Rende 2010; Abbott and Winzer-Serhan 2012; Clifford, Lang, and Chen 2012)).

Here, we report for the first time a direct interaction of Lypd6 with native human nAChRs from fresh human temporal cortical extracts and we identify Lypd6 as an inhibitor of nAChR function in rat hippocampal slices and PC12 cells. Since Lypd6 and nicotine both modulate nAChRs and also regulate developmental processes, we further sought to examine a possible interaction between the two in a developmental model of nicotine exposure, and show that nicotine administration to pregnant rats alters Lypd6 protein levels in the brain of the adult offspring.

Materials and Methods

Human tissue and animals

Human temporal neocortical tissue was obtained from an anterior temporal lobectomy performed in a patient (female, age 58) with medically intractable temporal lobe epilepsy with hippocampal onset. Written informed consent was obtained before surgery. The study was approved by the Ethical Committee in the Capital Region of Denmark (H-2-2011-104) and performed in accordance with the Declaration of Helsinki. The tissue was immediately frozen on dry ice and stored at −80°C until use.

Animal use for brain slice electrophysiology studies (Harlan Mice laboratories, Denmark) was permitted by the Animal Welfare Committee, appointed by the Danish Ministry of Justice and all experiments were in accordance with institutional guidelines (The European Communities Council Directive of 24 November 1986 (86/609/EEC) and with Danish laws regulating experiments on animals.

Pregnant dams and adult male Sprague Dawley (SD) rats (200–250 g) were obtained from Charles River Laboratories (Germany), and housed individually or two per cage, respectively. For the experiment with perinatal nicotine exposure timed-pregnant SD rats were obtained from Harlan Laboratories (Frederick, MD, USA). Pups were weaned at

postnatal day (PND) 21. Only male pups were analyzed in this study. Animal procedures were conducted with approval of the Howard University Animal Care and Use Committee (HU-IACUC) adhering to the guidelines set forth by the National Research Council, or in accordance with the Danish National Guide for Care and Use of Laboratory animals and the European Communities Council Directive of 24 November 1986 (86/609/EEC).

Mice deficient for the α7 or β2 nAChR subunit (C57BL/6J background), and wild type (WT) littermates were purchased from The Jackson Laboratories and bred at Virginia Commonwealth University. Mice deficient for the β4 nAChR subunit were obtained from Baylor University School of Medicine (Xu et al. 1999), and subsequently maintained at the University of Colorado. Brains from 8–12 weeks old male or female homozygous knockout (KO) and age- and sex-matched wild-type (WT) mice were used. Animals were kept on a 12/12 h light/dark cycle provided with standard rodent diet and water *ad libitum*. The male animals were acclimatized for a minimum of 7 days and the dams for about 24 hours after arrival before experiments began.

Developmental, tissue, cellular and subcellular distribution of Lypd6

Tissue cross-linking using the cell-impermeable cross-linking agent bis(sulfosuccinimidyl) suberate (BS^3, Pierce Biotechnology), fractionation into crude synaptosomes or soluble and membrane fractions, culturing of neuronal and astro- and microglia cultures, as well as the developmental study and sampling of cerebrospinal fluid has been described previously for the same samples that are being used in the present study (Thomsen et al. 2013).

mRNA extraction and qPCR

Total RNA was isolated using Trizol Reagent (Sigma-Aldrich) according to the manufacturer's instructions. RNA samples were dissolved in RNase-free water and RNA content was quantified using a Nanodrop ND-1000 Spectrophotometer (Nanodrop Technologies, Wilmington, DE). Samples were diluted with RNase-free water to equal RNA concentrations and reverse transcribed into single-stranded cDNA with Invitrogen™ SuperScript® III First-Strand Synthesis system (Thermo Fisher Scientific Inc.) according to the manufacturer's directions using 1,25 μM oligo$(dT)_{20}$ primers, 5 mM $MgCl_2$, and 2 units RNase inhibitor. Real-time qPCR reactions were performed in a total volume of 20 μl, containing 5 μl sample cDNA, 1x Precision Plus qPCR Master mix, premixed with SYBR-green (Primerdesign, Southampton, UK), and 16 pmol of the forward and reverse primers (DNA technology, Aarhus, Denmark). PCR was performed on a Light Cycler® 480 Real-Time PCR System (Roche, Indianapolis, IN) with a 2 minute preincubation at 95°C followed by 40 cycles of 15 seconds at 95°C, 10 seconds at 60°C and 10 seconds at 72°C. The primer pair for Lypd6 was (written 5′-3′): GCTACAAGATCTGCACCTCC and GCAAATGTGGCATCAGTGTC. Primer pairs were validated using serially diluted cDNA to establish a standard curve and by confirming the existence of a single product on a gel at the correct molecular weight. Quantification of mRNA expression was performed according to the comparative C_T method as described by (Schmittgen and Livak 2008). For each sample, the amount of target mRNA was normalized to the mean of the PND60 group.

Affinity purification

Recombinant human GST-tagged Lypd6 produced in E.coli (Cusabio, Wuhan, China) and dissolved to 1 mg/ml in PBS, pH 7.4 was coupled to PureProteome™ NHS Flexibind magnetic beads (Millipore, Billerica, MA) in a ratio of 1:2 (vol/vol) using the manufacturer's instructions. Successful coupling was confirmed by subsequent protein determination, showing a substantial decrease in the protein content of the Lypd6 solution. Another batch of beads without Lypd6 in the PBS was processed in parallel as a negative control. The beads were incubated in 0.1% bovine serum albumin in PBS, pH 7.4 for 1 hour at 4°C prior to use.

Approximately 100 mg human temporal neocortical tissue was lysed in 1 ml lysis buffer (50 mM Tris, 50 mM NaCl, 5 mM EDTA, 5 mM EGTA, 10 μl/ml protease inhibitor cocktail (Sigma-Aldrich, Brøndby, Denmark), pH 7.5) using a PT1200C polytron blender (Kinematica, Luzern, Switzerland) for 20 seconds. The lysate was centrifuged 30 minutes at 160,000 × g at 20–22°C using an air-driven ultracentrifuge (Airfuge®, Copenhagen, Denmark), and the supernatant discarded. The pellet was resuspended in 1 ml lysis buffer containing 2% Triton X-100 by blending for 20 seconds and incubated 2 hours at 4°C on a rotor (15 rpm). Thereafter, the sample was centrifuged as above and the resulting supernatant (Input) was used for affinity purification. Total protein content was determined using the Pierce 660nm Protein Assay (Thermo scientific, Rockford, IL) and 700–1000 μg protein was incubated with 50 μl magnetic beads in a total volume of 1500 μl lysis buffer for 18–22 hours at 4°C on a rotor (15 rpm). For experiments including α-bungarotoxin (α-BTX, Tocris Bioscience, Bristol, UK), the tissue was lysed in 10 ml lysis buffer and centrifugation was performed in 4°C. 100 nM α-BTX (final concentration) or vehicle (PBS) was added to the tissue extracts followed by incubation for 30 minutes on ice before addition of beads.

Subsequently, a sample of the remaining homogenate after affinity purification was taken (Output) and the beads were washed twice in 1 M NaCl, 8 mM Na_2HPO_4, 2 mM NaH_2PO_4, 0.5% Triton X-100, pH 7.5 and thrice in 0.1 M NaCl, 8 mM Na_2HPO_4, 2 mM NaH_2PO_4, 0.5% Triton X-100, pH 7.5 and immediately processed for western blotting.

PC12 cell culture and ERK phosphorylation assay

PC12 cells were maintained in 75 cm^2 flasks coated with 5 μg/ml poly-L-lysine (Sigma-Aldrich), in Dulbecco's modified Eagle medium (DMEM, Gibco Life Technologies, NY, USA) supplemented with 10% heat inactivated horse serum, 5% fetal bovine serum, 25 U/mL penicillin, 25 μg/mL streptomycin, 1 mM sodium pyruvate, and 2 mM glutamine at 37°C in a humidified incubator with 5% CO_2. Cells were subcultured every 3–4 days by detachment with 0.25% trypsin in EDTA solution (Gibco Life Technologies, NY, USA) and re-seeded at 15% confluence.

For the ERK phosphorylation assay, cells were seeded in 24-well plates at 12×10^4 cells/cm^2, 24 hours prior to the experiment. On the day of the experiment cells were incubated for 10 minutes with recombinant human Lypd6 protein or α-conotoxins PIA, MII or AuIB (Tocris Bioscience, Bristol, UK) diluted in DMEM, followed by 5 minutes stimulation with 25 μM nicotine (Sigma-Aldrich). Thereafter, cells were lysed in 100 μL ice cold lysis buffer/well

(100 mM NaCl, 25 mM EDTA, 10 mM Tris, 4 mM Na_3VO_4, 1 mM NaF, and 1 % (v/v) Triton X-100, 1 % (v/v) NP-40, 1 μL/mL protease inhibitor cocktail (Sigma-Aldrich), pH 7.4). Ensure complete lysis, lysates were then placed in -80°C for 15 minutes, thawed and sonicated for 5 seconds on ice. Lysates were stored at −80°C until use.

Nicotine administration

Nicotine was administered to pregnant rats through a mini-osmotic infusion pump (Model # 2006, Alzet, Cupertino, CA) surgically implanted between the scapulae at gestational day 7, as previously described (Hong Wang and Gondré-Lewis 2013; H Wang et al. 2011). Nicotine hydrogen tartrate (Sigma-Aldrich, St Louis, MO) was prepared fresh on the day of pump implantation and delivered to dams at a rate of 4 mg/kg/day (free base weight) from pregnancy until pups reached PND21. At PND21, the pups were weaned and allowed to reach adulthood (PND60). Hippocampus (HIP) and frontal cortex (FC) from male pups were microdissected and stored at −80°C for subsequent experimentation. Frontal cortical and hippocampal tissue from the left hemisphere were lysed for western blotting, and hippocampal tissue from the right hemisphere was used for BS^3 cross-linking and synaptosome preparations as above. To study the effect of nicotine when administered directly to young and adult rats, 0.4 mg/kg nicotine (free base weight) or vehicle (0.9% saline) was administered subcutaneously (s.c.) twice daily for 7 days (PND8–14 or 54–60) and the FC and HIP were dissected 4 hours after the last administration.

Western blotting

Total protein content was measured using a DC Protein Assay Kit (Biorad, Hercules, CA). Equal amounts of lysates were then diluted in loading buffer (final concentration: 60 mM Tris, 10% (v/v) glycerol, 5% (v/v) mercaptoethanol, 2% (w/v) SDS, 0.025% (w/v) bromophenol blue, pH 6.8), incubated for 5 minutes at 95°C and submitted to gel electrophoresis using AnykD™ gels (Biorad), and blotted onto PVDF membranes (BioRad). Membranes were washed in tris-buffered saline with 0.1% Tween 20(TBS-T) and blocked in TBS containing 5% (w/v) dry milk powder, which was also used for antibody incubations. Incubation in primary antisera against Lypd6 (1:1,000, #ARP53451_P050, Aviva Systems Biology, San Diego, CA), Lynx1 (1:1,000, #sc-23060, Santa Cruz Biotechnology, Heidelberg, Germany), Ly6H (1:1,000, #H00004062-M01, Novus Biologicals, Cambridge, UK), α3, α4, α5, α6 (1:100 #sc-1771, sc-5591, sc-28795, sc-27292 Santa Cruz Biotechnology) for which the selectivity has been previously characterized (Guan et al. 2001; Yu, Guan, and Nordberg 2007; Kabbani et al. 2007; Lang et al. 2003), β2 (1:1,000, provided by Dr. Cecilia Gotti) and α7, β4 (1:1,000 #ab23832 and 1:100 #ab156213 Abcam, Cambridge, UK) which we have validated in this study (Supplementary figure S3), Actin (1:10,000, #A5060, Sigma-Aldrich), GluR2 (1:200, #MABN71, Millipore), PSD-95 (1:2,000, #ab9708, Millipore), phosphorylated ERK1/2 (1:4,000 #9101 Cell Signaling, Leiden, the Netherlands) or ERK1 (1:4,000, #610031, BD Transduction Laboratories, Franklin Lakes, NJ) was done overnight at 4°C on parafilm in a humidified container, followed by 3×10 minute washes in TBS-T and 1 hour incubation at 20–22°C in horseradish peroxidase-conjugated secondary antibody (1:2,000, Dako, Glostrup, Denmark). After thorough washing in TBS-T, enhanced chemiluminescence Western blotting detection reagents (Western Lightning® ECL Pro, Perkin Elmer, Waltham, MA) were used for signal

detection and protein bands were visualized using an automated film developer (Colenta Labortechnik, Wiener Neustadt, Austria). Mean optical densities of bands were measured and their corresponding background measurement subtracted.

Brain slice preparation and Electrophysiology

Patch clamp, whole cell recordings were made from hippocampal CA1 interneurons in rat brain slices to determine the effects of Lypd6 on membrane current responses to nAChR agonists. Preparation of brain slices containing hippocampal CA1 neurons was conducted essentially as previously described (Soni and Kohlmeier 2015). Briefly, 12–15 day old NMRI wild-type mice of either sex were anesthetized with isofluorane, decapitated, and the brain was rapidly removed and placed into ice-cold (0–4°C) artificial cerebrospinal fluid (ACSF) which contained (in mM): 124 NaCl, 5 KCl, 1.2 Na_2HPO_4, 2.7 $CaCl_2$, 1.2 $MgSO_4$, 10 glucose and 2.6 $NaHCO_3$, bubbled with 95% O_2/5% CO_2 resulting in a pH of 7.4. The block of the brain containing the HIP was sectioned into 250 μm thick coronal slices using a vibrotome (Leica VT 1200S, Leica, Germany) after vertical deflection was minimized. Thereafter, slices containing the HIP were incubated in ACSF at 37°C for ~20 min followed by maintenance at room temperature for one hour to reach equilibration.

All recordings were conducted in a submersion recording chamber at room temperature. Whole-cell recordings were obtained from CA1 interneurons identified visually using an upright microscope (Olympus BX51WI, Germany). Recording pipettes were made from borosilicate glass capillary tubing (1.5 mm O.D), pulled on a horizontal puller (Sutter Instruments, P-95) and filled with internal patch solution (resistance of ~ 6 M′Ω) containing: (in mM) 144 K-gluconate, 3 $MgCl_2$, 10 HEPES, 0.3 NaGTP, and 4 Na_2ATP (295–300 mOsM). Membrane currents were recorded using an Axopatch-200B amplifier (Axon Instruments) and were filtered at 2 KHz (low-pass Bessel filter) at the amplifier output and digitized at 20 KHz, with subsequent analysis of current amplitudes performed with Clampex 10.3 (Molecular Devices, USA).

Membrane responses induced by activation of nAChRs on CA1 interneurons were recorded following application of nicotine (100 μM, Sigma, St. Louis, MO, USA), or the nAChR agonist, DMPP (50 mM, Sigma, MO, USA), in the absence or presence of human recombinant Lypd6 protein (6 μM, Cusabio, Wuhan, China). All agonists were applied from borosilicate micropipettes (~ 2 MΩ) using pressure delivered via a picospritzer III (Parker Hannifin Corporation, Mayfield Heights, OH, USA) at a distance of ≤100 μm from the recorded soma, with a constant pressure maintained at 10 psi for 10–50 msec. Lypd6 was also applied using a borosilicate micropipette (~ 500KΩ) using pressure delivered via a picospritzer III at a distance of ~ 200 μm from recorded somas, with a constant pressure maintained at 10 psi for a duration of 4–5 sec. During Lypd6 application, bath perfusion of ACSF was stopped for 3–4 min in order to maximize the diffusion of Lypd6 into the slice. To check the specificity of Lypd6-dependent effects on nAChR responses, the order of drug application was reversed in a few recordings, such that slices were exposed to Lypd6, then nAChR agonists were applied.

Statistical analysis

Data were analyzed using two-way ANOVA with Sidak-corrected multiple comparisons or Bonferroni-corrected ratio paired t-tests. For the electrophysiological recordings, data were analyzed using unpaired or paired t-tests. The statistical calculations were performed using GraphPad Prism version 6 for Windows (GraphPad Software, San Diego, CA). All data are presented as mean ± standard error of the mean, and a *P*-value of less than 0.05 was considered statistically significant.

Results

Distribution and developmental expression of Lypd6

To characterize the expression pattern of Lypd6, we analyzed Lypd6 protein levels in different organs of adult male rats using western blotting. A band corresponding to Lypd6 protein was detected in all organs analyzed with high levels in the cortex and cerebellum of the brain, moderate levels in lung, kidney, and liver, and low levels in the heart and prostate (Figure 1A). In the kidney, the Lypd6 antibody detected an additional lower molecular weight band.

We further detected high levels of endogenous Lypd6 protein in rat primary cortical neurons cultured to 14 DIV (Figure 1B). Cortical neurons cultured to 7 DIV and astroglia cultured to 18DIV displayed moderate staining, whereas Lypd6 was not detectable in primary microglia cultured to 15DIV.

Previous studies have shown that Lynx proteins are expressed as GPI-anchored membrane proteins, but may also exist as soluble proteins (Bamezai 2004; Adermann et al. 1999). Fractionation of rat cortical tissue into soluble and membrane fractions by ultracentrifugation and subsequent western blotting alongside samples of rat cerebrospinal fluid (CSF) revealed that Lypd6 was detectable in the membrane fraction, but not in the soluble fraction or in CSF samples (Figure 1C). To validate the separation, we demonstrated that the membrane-associated scaffolding protein, postsynaptic density 95 (PSD-95), and the AMPA receptor subunit GluR2 were only present in the membrane fraction, whereas the soluble protein ERK1 was only present in the soluble fraction.

To determine the subcellular localization of Lypd6, tissue homogenates from the FC and HIP were fractionated into nuclear (P1) and synaptosomal (P2) fractions (Figure 1D). There was a significantly higher level of Lypd6 in the HIP synaptosomal fraction compared to the total homogenate ($P<0.01$). Additionally, comparing the synaptosomal and nuclear/endosomal fractions revealed a significantly higher level of Lypd6 in synaptosomes in both the FC and HIP (both $P<0.05$). GluR2 was used as a positive control as it is known to be located in the synaptosomal fraction (Srivastava et al. 1998).

To determine the extent of surface expression of Lypd6, protein levels in tissue extracts from the FC or HIP of adult rats, cross-linked using the cell-impermeable protein cross-linking agent BS^3, were compared with untreated extracts (Figure 1E), and the GluR2 receptor subunit was used as a positive control and reference value (Grosshans et al. 2002; Mielke and Mealing 2009; Carino et al. 2012). In the HIP, the Lypd6 signal was reduced by 42

± 0.07 % (mean ± SEM, $P < 0.01$) compared to non-cross-linked tissue extracts, corresponding to 87% of the signal reduction seen with GluR2, showing that Lypd6 is predominantly present on the cell surface. In the FC, the Lypd6 signal was reduced by 24 ± 0.11%, but was not significantly different from vehicle controls.

We finally studied the expression pattern of Lypd6 during development. We measured Lypd6 mRNA levels in the FC and HIP of rats at PND1, 7, 14, 26, 42, and 60 (Figure 1F). Lypd6 mRNA was present in in the FC at birth, but decreased to PND26 with a slower decrease from PND26 until PND60. In the hippocampal formation, Lypd6 mRNA was detected at high levels at birth and the levels decreased to near adult levels within the first 3 postnatal weeks.

Taken together, these data indicate that Lypd6 is a membrane-bound protein, predominantly expressed in the rodent brain and highly enriched at the synaptic loci.

Lypd6 binds to multiple nAChRs in human brain extracts

Members of the Lynx family have been demonstrated to bind to nAChRs altering their function (Ibañez-Tallon et al. 2002; Tekinay et al. 2009; M. M. Jensen et al. 2015). To test the binding of Lypd6 for nAChR subunits we performed affinity purification using bead-coupled recombinant human Lypd6 as bait. In extracts from human temporal cortex Lypd6 co-purified with α3, α4, α5, α6, α7, β2, and β4 nAChR subunits (Figure 2A), but not with GluR2. None of the nAChR subunits were detected when the affinity purification was performed using non-coupled beads, confirming that co-purification of nAChR subunits was attributable to a specific interaction with Lypd6. The selectivity of α7, β2, and β4 nAChR subunit antibodies used was verified by performing affinity purification with human recombinant Lypd6-coupled beads on α7, β2, and β4 KO mice cortical tissue, showing that each of the subunits was only detected in the corresponding WT, but not KO homogenates (supplementary figure S3). Although quantitative assessment is not possible due to a low sample number, visual comparison of the input and output homogenates from the affinity purification suggest a reduction in band intensity for α4, α6, and α7, indicating that a detectable proportion of these nAChR subunits have been co-purified by Lypd6.

Pre-incubation of human temporal cortical extracts with the α7-specific orthosteric antagonist α-BTX (100 nM) significantly reduced the amount of the α7 nAChR subunit (26.8 ± 0.04 %, $P<0.01$) isolated during the Lypd6 affinity purification compared to pre-incubation with PBS, whereas it did not significantly affect the amount of α3, α4, α5, α6, β2 or β4 purified (Figure 2B, C). These results suggest that Lypd6 is able to interact with several nAChR subunits in the human cortex, and that Lypd6 competes with α-BTX for binding to the α7 nAChR.

Lypd6 regulates nicotine-induced ERK phosphorylation

To further assess the functional effect of Lypd6 binding to nAChRs, we used rat pheochromocytoma PC12 cells that natively express nAChRs (Nakayama et al. 2006). Stimulation with 25 μM nicotine significantly increased phosphorylation of the MAP kinase ERK in PC12 cells. This increase was completely inhibited by pre-incubation with 4 μM recombinant human Lypd6 (Figure 3). Lower concentrations of recombinant Lypd6 (0.04

and 0.4 μM) also slightly reduced ERK phosphorylation, but this did not reach significance. Lypd6 exposure alone did not affect basal levels of ERK phosphorylation. We have previously shown that the effect of nicotine on ERK phosphorylation in the PC12 cell line we used here is depend on α3β4-containing nAChRs (Arvaniti, Mikkelsen, and Thomsen 2015).

Lypd6 attenuates nicotine-induced hippocampal inward currents

Whole-cell recordings were obtained from visually identified hippocampal CA1 interneurons (Alkondon and Albuquerque 2001; Freund and Buzsáki 1996) of stratum oriens and stratum radiatum, where these interneurons have horizontally oriented spindle-shaped cell bodies and this feature is characteristically distinct from pyramidal neurons (Figure 4A). Hippocampal interneurons where chosen due to the abundant expression of the α7 nAChR subtype (Frazier et al. 1998; Buhler and Dunwiddie 2001; Buhler and Dunwiddie 2002).

Lypd6, when applied alone, did not induce an outward or inward membrane current (Figure 4B). When held at −60 mV, nicotine application (100μM, 10–50 msec duration) resulted in an inward current of 67.2 ± 22.0 pA, which was repeatable with an interval of at least 3 minutes between nicotine applications (n=5, Figure 4C, D). In presence of Lypd6 (6 μM), the average reduction of nicotine-induced inward currents in each individual neuron was 57.4 ± 15.2 % (mean ± SEM, paired t-test, $P < 0.01$, $n_{cells}=5$, Fig. 4E). Similarly, the non-specific nAChR agonist, DMPP (50 μM) induced an average inward current of 29.7±7.2 pA, which was attenuated by 74.8 ± 12.6 % when DMPP was applied in presence of Lypd6 ($n_{cells}=3$, t-test, $P < 0.05$; Figure 4E).

We further examined whether Lypd6–mediated attenuation of inward currents was due to order effects, or run down of nAChR responses due to cellular exhaustion. After pre-incubation with Lypd6, nicotine was applied repeatedly, with a recovery time in between applications of ~3 minutes (Figure 4D). A gradual increase in the amplitude of nicotine-induced inward currents was noted, suggesting that the observed effect was associated only with the presence of Lypd6 and could be reversed.

Perinatal nicotine exposure increases Lypd6 levels

We analyzed the protein levels of Lypd6, Lynx1, and Ly6H at PND7, 21, and 60 in the FC and HIP of male rats exposed to continuous infusion of nicotine via osmotic minipumps implanted into the pregnant dams (Figure 5A, B).

A two-way ANOVA with age and treatment as the fixed factors revealed a significant main effect of nicotine treatment on Lypd6 levels in the HIP ($P<0.01$), but did not reach significance in the FC ($P=0.07$). A subsequent Sidak-corrected multiple comparison on HIP samples showed that nicotine significantly increased Lypd6 levels at PND60 (Figure 5A). A main effect of nicotine was also demonstrated on β2 levels in the FC ($P<0.01$), where a multiple comparisons test showed a significant effect of nicotine on β2 levels at PND21. Two-way ANOVAs on Lynx1 or Ly6H levels showed no significant main effect of nicotine.

To further characterize the effect of nicotine on hippocampal Lypd6 levels, we demonstrate that nicotine administration significantly increased Lypd6 levels in the putative nuclear

fraction (P1, $P<0.05$), whereas there was no difference between the groups in synaptosomal fractions (P2) or on Lypd6 surface levels, as measured using BS^3 cross-linking of proteins (Figure 5C). To validate the methods, we show that GluR2 is reduced by cross-linking and increased in synaptosomes in the two groups. Administration of nicotine (0.4 mg/kg s.c. twice daily for 7 days) to young or adult rats, did not alter protein levels of Lypd6, Lynx1, or Ly6H in the FC or HIP (Figure 6).

Moreover, Lypd6, Lynx1, and Ly6H protein levels in FC from wild-type and β2, α7, or β4 knock-out mice were compared using unpaired t-tests. No significant differences were found after genetic deletion of these nAChR subunits (Figure 7).

Discussion

Here, we show that recombinant Lypd6 binds to multiple nAChR subunits in the human brain and inhibits nicotine-mediated activation of nAChRs *in vitro*. Furthermore, perinatal nicotine administration leads to increased hippocampal Lypd6 protein levels in adulthood. These results suggest that Lypd6 modifies cholinergic neurotransmission by a direct interaction with mature nAChRs in the brain, and that this regulation may be altered by maternal exposure to nicotine.

Lypd6 is situated to regulate neurotransmission in the brain

Lypd6 protein was detectable in all organs examined and had a high expression in the brain. The ubiquitous expression of Lypd6 protein is in accordance with Lypd6 mRNA expression in human and mouse organs (Zhang et al. 2010; Darvas et al. 2009). In primary cultures, Lypd6 is expressed by neurons and astroglia, but not by microglia. We have previously demonstrated that the Lynx proteins Lynx1 and Ly6H are exclusively expressed in neurons (Thomsen et al. 2013), but other Lynx proteins have also been detected in glia (Tanaka, Marunouchi, and Sawada 1997; Mildner et al. 2007; Cray et al. 1990; Rogers et al. 1996).

Lynx proteins may exist as GPI-anchored membrane proteins or soluble proteins (Bamezai 2004; Adermann et al. 1999). We detected Lypd6 in membrane fractions, but not soluble fractions or CSF samples and found that Lypd6 was predominantly localized to synaptosomes in the rat cortex, suggesting that Lypd6 is a membrane protein involved in synaptic function. This is in line with *in silico* analysis of the *Lypd6* gene in zebrafish, showing that it contains a possible GPI-attachment site, as well as studies in both zebrafish embryos and a mammalian cell line, showing that Lypd6 is GPI-anchored on the cell membrane (Özhan et al. 2013). In contrast, other members of the Lynx family such as the prostate stem cell antigen (PSCA) are detected only in the soluble fraction (M. M. Jensen et al. 2015). This discrimination may underlie differences in the mode of action, as a soluble version of the Lynx protein Lynx1 has been shown to exert a distinctive phenotype compared to the full-length form, when expressed in a transgenic mouse model (Julie M Miwa and Walz 2012).

We further found that Lypd6 mRNA is highly expressed during early development, showing high levels in the first postnatal days in rat CTX and HIP, followed by a decrease towards adulthood. Our results imply a potential crucial role for Lypd6 in early mammalian

development and support previous data, showing Lypd6 to be essential in vertebrate embryogenesis, by being involved in mesoderm and neuroectoderm patterning in zebrafish gastrulation (Özhan et al. 2013). In addition, the developmental expression pattern of several other Lynx proteins in the brain, such as Lynx1, Lynx2 or Ly6H, as well as the involvement of Lynx1 in the regulation of plasticity in the visual cortex further support a role of this protein family in development (Dessaud et al. 2006; Thomsen et al. 2013; Morishita et al. 2010).

Lypd6 binds to and regulates nAChRs

We detected co-purification of α3, α4, α5, α6, α7, β2, and β4 nAChR subunits by affinity pull-down from human cortical extracts, using recombinant human Lypd6. This is the first demonstration of a direct interaction between a Lynx protein and native nAChRs in the human brain. These data indicate that Lypd6 protein is able to bind to multiple nAChR subunits in the human brain, including the clinically relevant α7 nAChR (reviewed in (Thomsen and Mikkelsen 2012)). We have previously shown that a soluble version of Lynx1 also binds multiple nAChR subunits (Thomsen et al. 2014), but this broad spectrum of binding is not a feature of all Lynx proteins, as SLURP-1 has been shown, using the same method, to bind selectively to α7 nAChRs (Lyukmanova et al. 2016).

To specifically investigate the interaction between Lypd6 and the human α7 nAChR, we used α-BTX and showed that it can interfere with α7 binding to Lypd6. This suggests that Lypd6 binds orthosterically to α7 nAChRs, although we cannot exclude the possibility that binding of α-BTX leads to conformational changes on the α7 nAChR, changing its affinity for Lypd6. If indeed Lypd6 binds on the orthosteric site, it indicates that Lypd6 could act as an antagonist, rather than an allosteric modulator, of nAChR function. In contrast, Lynx1 does not compete with α-BTX for binding to human α7 nAChRs or with epibatidine for binding to α4β2 nAChRs, suggesting that it binds outside of the orthosteric binding site (Lyukmanova et al. 2011).

The direct binding between Lypd6 and nAChRs prompted us to ask whether this had an effect on nAChR function. We show that a soluble version of Lypd6 completely inhibits nicotine-induced phosphorylation of ERK in PC12 cells and reversibly attenuates nicotine-induced inward currents in hippocampal interneurons of rat brain slices. This is in line with previous studies, indicating a modulatory role of Lynx proteins on whole-cell currents (Lyukmanova et al. 2016; Puddifoot et al. 2015; Wu et al. 2015; Ibañez-Tallon et al. 2002; J MMiwa et al. 1999). Notably, Lypd6 exposure did not affect the baseline membrane current or basal levels of ERK phosphorylation, suggesting that the inhibitory effect is specifically related to nAChR signaling and that Lypd6 is not able to activate nAChRs. Activation of the ERK/MAPK pathway by phosphorylation is an important step in the formation of LTP and memory in the HIP (Adams and Sweatt 2002), and nicotine-mediated enhancement of LTP in the HIP is dependent on ERK (Welsby, Rowan, and Anwyl 2009). In accordance with previous findings (Nakayama et al. 2006), we have shown that this effect of nicotine in PC12 cells is dependent on α3β4-containing nAChRs (Arvaniti, Mikkelsen, and Thomsen 2015), suggesting that Lypd6 affects the function of α3β4-containing nAChRs. This is not to say, however, that the effects of Lypd6 in the brain are restricted to α3β4-containing nAChRs.

Our results suggest that Lypd6 can act as an endogenous orthosteric antagonist of nAChRs in the brain. This sets Lypd6 apart from other Lynx proteins, such as Lynx1 and Lynx2, which have been shown to bind to and negatively regulate the function of α7 and α4β2 nAChRs in heterologous expression systems (Ibañez-Tallon et al. 2002; Tekinay et al. 2009), suggesting an allosteric mode of action. However, we have employed a soluble variant of Lypd6 that could possibly function differently than, or bind to sites otherwise unreachable by, endogenous GPI-anchored Lypd6 on nAChRs, as previously speculated for the soluble Lynx1 protein (Julie M Miwa and Walz 2012).

It has previously been shown that transgenic overexpression of Lypd6 in mice increases nicotine-induced calcium currents and enhances behaviours associated with cholinergic neurotransmission (Darvas et al. 2009). Our finding that Lypd6 forms a stable complex with nAChRs suggests that these effects may be caused by a direct interaction between Lypd6 and nAChRs. The apparent discrepancy between an enhancement of calcium currents and a decrease in inward currents and phosphorylation of ERK by Lypd6 may be explained by the experimental setups. We have employed a short exposure to a soluble variant of Lypd6, which likely affects primarily surface nAChRs, and which might bind differently to nAChRs compared with endogenous Lypd6. Transgenic overexpression of Lypd6, on the other hand, may have more complex effects, possibly involving chaperoning of nAChRs by Lypd6 in the endoplasmic reticulum, as has previously been demonstrated for the Lynx proteins Lynx1 and Ly6H (Nichols et al. 2014; Puddifoot et al. 2015). Lypd6 protein is primarily intracellular when overexpressed in COS-7 cells (Zhang et al. 2010), which is in line with a potential intracellular function of Lypd6 after transgenic expression. We demonstrate that endogenous Lypd6 is predominantly located on the cell surface in the rat HIP, whereas this localization is not as pronounced in the FC. Given the potential opposing function of surface vs. intracellular Lypd6, this differential subcellular distribution of Lypd6 may have a significant impact on the function of Lypd6 in different brain regions.

Nicotine regulates hippocampal Lypd6 levels

Since nicotine and Lypd6 both affect nAChR function as well as early development, we found it pertinent to examine whether exposure to nicotine during development affected Lypd6 protein levels in the brain. Using an exposure paradigm known to result in stable plasma levels of nicotine corresponding to that found in light to moderate smokers (Matta et al. 2007), we found that perinatal nicotine exposure to dams produced an almost 2-fold increase of Lypd6 in the HIP of the adult offspring, whereas there were no effects on the Lynx proteins Lynx1 and Ly6H. This suggests that nicotine has long term effects on Lypd6 expression.

Maternal smoking during or after pregnancy can have long term detrimental effects on the development of the offspring and lead to lifelong impairments (Blood-Siegfried and Rende 2010; Abbott and Winzer-Serhan 2012; Clifford, Lang, and Chen 2012). Prenatal nicotine exposure reduces hippocampal levels of phosphorylated ERK in rats, and this has been suggested to underlie the cognitive deficits observed after gestational nicotine exposure (Parameshwaran et al. 2013). We find that Lypd6 inhibits nAChR-mediated ERK phosphorylation *in vitro* and that perinatal nicotine administration increases Lypd6 levels,

suggesting that decreased ERK phosphorylation after prenatal nicotine administration may be caused by increased inhibition of nAChRs by Lypd6. It is therefore possible that part of the detrimental effect of nicotine on the development of the offspring is due to dysregulation of Lypd6.

We further showed that the increase in Lypd6 following nicotine exposure was primarily evident in a putative nuclear/endosomal fraction, but not in synaptosomes, suggesting that nicotine leads to a preferential increase in non-synaptic Lypd6. If Lypd6 is able to chaperone nAChRs, nicotine administration might therefore alter this chaperoning. The effect of nicotine on Lypd6 levels was not recapitulated by nicotine administration to young or adult rats, suggesting that Lypd6 is more susceptible to regulation by nicotine during early development.

Nicotine administration upregulates nAChRs in the brain, including the α3β4 subtype (Govind, Vezina, and Green 2009; Mazzo et al. 2013). We therefore hypothesized that the effect of nicotine exposure on Lypd6 protein levels was an indirect effect caused by upregulation of nAChRs. However, genetic ablation of β2-, β4-, or α7-containing nAChRs did not affect Lypd6 levels, suggesting that decreasing the levels of the major nAChR subtypes in the brain does not affect Lypd6 protein levels. It is, however, shown that Lynx1 interacts preferentially with α4/α4 dimers in α4β2 nAChRs (Nichols et al. 2014), and if Lypd6 preferentially binds to α/α interfaces as well, we cannot exclude a potential effect of nicotine via α-subunit upregulation, other than α7. In a further attempt to see whether cholinergic tone or physiological changes affected Lypd6 signaling, we investigated regulation of Lypd6 by environmental enrichment in mice as well as by acute or repeated exercise training (Figure S1). Lypd6 levels were unchanged in these paradigms, suggesting at least some selectivity in the effect of nicotine on Lypd6 levels. Together with a lack of effect of knock-out of nAChR subunits on Lypd6 levels, these data suggest that the effect of nicotine on Lypd6 is not dependent on nAChR levels or cholinergic tone in adult animals. It thus seems the regulation of Lypd6 by nicotine is limited to a certain time window during early development.

Wnt/β-catenin signaling is important for early development, but also regulates nAChR localization and synaptic plasticity in the adult *C. elegans* nervous system (M. Jensen et al. 2012). Since both nicotine and Lypd6 protein can regulate the Wnt/β-catenin pathway (Zhou et al. 2013; Özhan et al. 2013), it is possible that nicotine affects Lypd6 levels via the Wnt/β-catenin pathway.

In summary, our results indicate that Lypd6 is an endogenous orthosteric antagonist of cholinergic signaling in the brain, and that it is dysregulated by nicotine exposure during early development. This suggests that part of the detrimental consequences of maternal nicotine exposure during and after gestation on development of the offspring may be due to dysregulation of Lypd6 levels.

Supplementary Material

Refer to Web version on PubMed Central for supplementary material.

Acknowledgments

The authors would like to thank Maria Nørnberg and Christine Andersen for providing technical assistance, Dr. Michael J. Marks for kindly providing tissue from transgenic mice, and Dr. Cecilia Gotti for kindly providing the β2 antiserum. This work was supported by the Danish Ministry of Science, Innovation and Higher Education, The Augustinus Foundation, Agnes and Pouls Friis Foundation, Fonden til Lægemiddelvidenskabens Fremme, the Danish Strategic Research Council (COGNITO), the Danish Council for Independent Research (DFF-4183-00246), The Danish Ministry of Culture, the Lundbeck Foundation, the National Institute of Neurological Disorders and Stroke, National Institutes of Health (NIH), NS65035, and the National Institute of Alcohol Abuse and Alcoholism (NIAAA), NIH AA021262.

References

Abbott, Louise C.; Winzer-Serhan, Ursula H. Smoking during Pregnancy: Lessons Learned from Epidemiological Studies and Experimental Studies Using Animal Models. Critical Reviews in Toxicology. 2012; 42(4):279–303. DOI: 10.3109/10408444.2012.658506 [PubMed: 22394313]

Adams, Paige J.; Sweatt, J David. Molecular Psychology: Roles for the ERK MAP Kinase Cascade in Memory. Annual Review of Pharmacology and Toxicology. 2002; 42(1):135–63. DOI: 10.1146/annurev.pharmtox.42.082701.145401

Adermann K, Wattler F, Wattler S, Heine G, Meyer M, Forssmann WG, Nehls M. Structural and Phylogenetic Characterization of Human SLURP-1, the First Secreted Mammalian Member of the Ly-6/uPAR Protein Superfamily. Protein Science. 1999; 8(4):810–19. DOI: 10.1110/ps.8.4.810 [PubMed: 10211827]

Alkondon M, Albuquerque EX. Nicotinic Acetylcholine Receptor alpha7 and alpha4beta2 Subtypes Differentially Control GABAergic Input to CA1 Neurons in Rat Hippocampus. Journal of Neurophysiology. 2001; 86(6):3043–55. [PubMed: 11731559]

Arvaniti, Maria; Mikkelsen, Jens D.; Thomsen, Morten S. Beta-Amyloid and Lypd6 Compete for Binding to Nicotinic Acetylcholine Receptors in Human Brain Extracts. Society for Neuroscience Annual Meeting; Chicago, IL: 2015.

Bamezai, Anil. Mouse Ly-6 Proteins and Their Extended Family: Markers of Cell Differentiation and Regulators of Cell Signaling. Archivum Immunologiae et Therapiae Experimentalis. 2004; 52(4):255–66. [PubMed: 15467490]

Blood-Siegfried, Jane; Rende, Elizabeth K. Journal of Midwifery & Women's Health. Vol. 55. Elsevier Ltd; 2010. The Long-Term Effects of Prenatal Nicotine Exposure on Neurologic Development; p. 143-52.

Buhler AV, Dunwiddie TV. Regulation of the Activity of Hippocampal Stratum Oriens Interneurons by α7 Nicotinic Acetylcholine Receptors. Neuroscience. 2001; 106(1):55–67. DOI: 10.1016/S0306-4522(01)00257-3 [PubMed: 11564416]

Buhler AV, Dunwiddie TV. Alpha 7 Nicotinic Acetylcholine Receptors on GABAergic Interneurons Evoke Dendritic and Somatic Inhibition of Hippocampal Neurons. J Neurophysiol. 2002; 87(1):548–57. [PubMed: 11784770]

Carino, Charlene; Fibuch, Eugene E.; Mao, Li-Min; Wang, John Q. Dynamic Loss of Surface-Expressed AMPA Receptors in Mouse Cortical and Striatal Neurons during Anesthesia. Journal of Neuroscience Research. 2012; 90(1):315–23. DOI: 10.1002/jnr.22749 [PubMed: 21932367]

Chung, Brian HY.; Mullegama, Sureni; Marshall, Christian R.; Lionel, Anath C.; Weksberg, Rosanna; Dupuis, Lucie; Brick, Lauren. European Journal of Human Genetics: EJHG. Vol. 20. Nature Publishing Group; 2012. Severe Intellectual Disability and Autistic Features Associated with Microduplication 2q23.1; p. 398-403.

Clifford, Angela; Lang, Linda; Chen, Ruoling. Neurotoxicology and Teratology. Vol. 34. Elsevier Inc; 2012. Effects of Maternal Cigarette Smoking during Pregnancy on Cognitive Parameters of Children and Young Adults: A Literature Review; p. 560-70.

Cray C, Keane RW, Malek TR, Levy RB. Regulation and Selective Expression of Ly-6A/E, a Lymphocyte Activation Molecule, in the Central Nervous System. Brain Research Molecular Brain Research. 1990; 8(1):9–15. [PubMed: 2166206]

Darvas, Martin; Morsch, Marco; Racz, Ildiko; Ahmadi, Seifollah; Swandulla, Dieter; Zimmer, Andreas. European Neuropsychopharmacology: The Journal of the European College of Neuropsychopharmacology. Vol. 19. Elsevier B.V. and ECNP; 2009. Modulation of the Ca2+ Conductance of Nicotinic Acetylcholine Receptors by Lypd6; p. 670-81.

Demars, Michael P.; Morishita, Hirofumi. Cortical Parvalbumin and Somatostatin GABA Neurons Express Distinct Endogenous Modulators of Nicotinic Acetylcholine Receptors. Molecular Brain. 2014; 7(1):75.doi: 10.1186/s13041-014-0075-9 [PubMed: 25359633]

Dessaud, Eric; Salaün, Danièle; Gayet, Odile; Chabbert, Marie; deLapeyrière, Odile. Identification of lynx2, a Novel Member of the Ly-6/neurotoxin Superfamily, Expressed in Neuronal Subpopulations during Mouse Development. Molecular and Cellular Neurosciences. 2006; 31(2): 232–42. DOI: 10.1016/j.mcn.2005.09.010 [PubMed: 16236524]

Frazier CJ, Rollins YD, Breese CR, Leonard S, Freedman R, Dunwiddie TV. Acetylcholine Activates an Alpha-Bungarotoxin-Sensitive Nicotinic Current in Rat Hippocampal Interneurons, but Not Pyramidal Cells. The Journal of Neuroscience. 1998; 18(4):1187–95. [PubMed: 9454829]

Freund TF, Buzsáki G. Interneurons of the Hippocampus. Hippocampus. 1996; 6(4):347–470. DOI: 10.1002/(SICI)1098-1063(1996)6:4<347::AID-HIPO1>3.0.CO;2-I [PubMed: 8915675]

Fu, Xiao Wen; Rekow, Stephen S.; Spindel, Eliot R. The Ly-6 Protein, lynx1, Is an Endogenous Inhibitor of Nicotinic Signaling in Airway Epithelium. American Journal of Physiology Lung Cellular and Molecular Physiology. 2012; 303(8):L661–68. DOI: 10.1152/ajplung.00075.2012 [PubMed: 22923641]

Govind, Anitha P.; Vezina, Paul; Green, William N. Nicotine-Induced Upregulation of Nicotinic Receptors: Underlying Mechanisms and Relevance to Nicotine Addiction. Biochemical Pharmacology. 2009; 78(7):756–65. DOI: 10.1016/j.bcp.2009.06.011 [PubMed: 19540212]

Grosshans DR, Clayton DA, Coultrap SJ, Browning MD. LTP Leads to Rapid Surface Expression of NMDA but Not AMPA Receptors in Adult Rat CA1. Nature Neuroscience. 2002; 5(1):27–33. DOI: 10.1038/nn779 [PubMed: 11740502]

Guan, Zhi-Zhong; Zhang, Xiao; Ravid, Rivka; Nordberg, Agneta. Decreased Protein Levels of Nicotinic Receptor Subunits in the Hippocampus and Temporal Cortex of Patients with Alzheimer's Disease. Journal of Neurochemistry. 2001; 74(1):237–43. DOI: 10.1046/j.1471-4159.2000.0740237.x [PubMed: 10617125]

Ibañez-Tallon, Inés; Miwa, Julie M.; Wang, Hai Long; Adams, Niels C.; Crabtree, Gregg W.; Sine, Steven M.; Heintz, Nathaniel. Novel Modulation of Neuronal Nicotinic Acetylcholine Receptors by Association with the Endogenous Prototoxin lynx1. Neuron. 2002; 33(6):893–903. [PubMed: 11906696]

Jensen, Majbrit M.; Arvaniti, Maria; Mikkelsen, Jens D.; Michalski, Dominik; Pinborg, Lars H.; Härtig, Wolfgang; Thomsen, Morten S. Neurobiology of Aging. Elsevier Inc; 2015. Prostate Stem Cell Antigen Interacts with Nicotinic Acetylcholine Receptors and Is Affected in Alzheimer's Disease; p. 2-11.

Jensen, Michael; Hoerndli, Frédéric J.; Brockie, Penelope J.; Wang, Rui; Johnson, Erica; Maxfield, Dane; Francis, Michael M.; Madsen, David M.; Maricq, Andres V. Wnt Signaling Regulates Acetylcholine Receptor Translocation and Synaptic Plasticity in the Adult Nervous System. Cell. 2012; 149:173–87. DOI: 10.1016/j.cell.2011.12.038 [PubMed: 22464329]

Kabbani, Nadine; Woll, Matthew P.; Levenson, Robert; Lindstrom, Jon M.; Changeux, Jean-Pierre. Intracellular Complexes of the beta2 Subunit of the Nicotinic Acetylcholine Receptor in Brain Identified by Proteomics. Proceedings of the National Academy of Sciences of the United States of America. 2007; 104(51):20570–75. DOI: 10.1073/pnas.0710314104 [PubMed: 18077321]

Lang PM, Burgstahler R, Sippel W, Irnich D, Schlotter-Weigel B, Grafe P. Characterization of Neuronal Nicotinic Acetylcholine Receptors in the Membrane of Unmyelinated Human C-Fiber Axons by in Vitro Studies. Journal of Neurophysiology. 2003; 90(5):3295–3303. DOI: 10.1152/jn.00512.2003 [PubMed: 12878715]

Lyukmanova, Ekaterina N.; Shenkarev, Zakhar O.; Shulepko, Mikhail A.; Mineev, Konstantin S.; D'Hoedt, Dieter; Kasheverov, Igor E.; Filkin, Sergey Yu, et al. NMR Structure and Action on Nicotinic Acetylcholine Receptors of Water-Soluble Domain of Human LYNX1. The Journal of Biological Chemistry. 2011; 286(12):10618–27. DOI: 10.1074/jbc.M110.189100 [PubMed: 21252236]

Lyukmanova, Ekaterina N.; Shulepko, Mikhail A.; Kudryavtsev, Denis; Bychkov, Maxim L.; Kulbatskii, Dmitrii S.; Kasheverov, Igor E.; Astapova, Maria V. Human Secreted Ly-6/uPAR Related Protein-1 (SLURP-1) Is a Selective Allosteric Antagonist of α7 Nicotinic Acetylcholine Receptor. Plos One. 2016; 11(2):e0149733.doi: 10.1371/journal.pone.0149733 [PubMed: 26905431]

Matta, Shannon G.; Balfour, David J.; Benowitz, Neal L.; Boyd, R Thomas; Buccafusco, Jerry J.; Caggiula, Anthony R.; Craig, Caroline R., et al. Guidelines on Nicotine Dose Selection for in Vivo Research. Psychopharmacology. 2007; 190(3):269–319. DOI: 10.1007/s00213-006-0441-0 [PubMed: 16896961]

Mazzo, Francesca; Pistillo, Francesco; Grazioso, Giovanni; Clementi, Francesco; Borgese, Nica; Gotti, Cecilia; Colombo, Sara Francesca. Nicotine-Modulated Subunit Stoichiometry Affects Stability and Trafficking of α3β4 Nicotinic Receptor. The Journal of Neuroscience: The Official Journal of the Society for Neuroscience. 2013; 33(30):12316–28. DOI: 10.1523/JNEUROSCI.2393-13.2013 [PubMed: 23884938]

Mielke, John G.; Mealing, Geoffrey AR. Cellular Distribution of the Nicotinic Acetylcholine Receptor alpha7 Subunit in Rat Hippocampus. Neuroscience Research. 2009; 65(3):296–306. DOI: 10.1016/j.neures.2009.08.003 [PubMed: 19682509]

Mildner, Alexander; Schmidt, Hauke; Nitsche, Mirko; Merkler, Doron; Hanisch, Uwe-Karsten; Mack, Matthias; Heikenwalder, Mathias; Brück, Wolfgang; Priller, Josef; Prinz, Marco. Microglia in the Adult Brain Arise from Ly-6ChiCCR2+ Monocytes Only under Defined Host Conditions. Nature Neuroscience. 2007; 10(12):1544–53. DOI: 10.1038/nn2015 [PubMed: 18026096]

Miwa JM, Ibanez-Tallon I, Crabtree GW, Sánchez R, Sali A, Role LW, Heintz N. lynx1, an Endogenous Toxin-like Modulator of Nicotinic Acetylcholine Receptors in the Mammalian CNS. Neuron. 1999; 23(1):105–14. [PubMed: 10402197]

Miwa, Julie M.; Freedman, Robert; Lester, Henry A. Neuron. Vol. 70. Elsevier Inc; 2011. Neural Systems Governed by Nicotinic Acetylcholine Receptors: Emerging Hypotheses; p. 20-33.

Miwa, Julie M.; Lester, Henry A.; Walz, Andreas. Optimizing Cholinergic Tone through Lynx Modulators of Nicotinic Receptors: Implications for Plasticity and Nicotine Addiction. Physiology (Bethesda, Md). 2012; 27(4):187–99. DOI: 10.1152/physiol.00002.2012

Miwa, Julie M.; Stevens, Tanya R.; King, Sarah L.; Caldarone, Barbara J.; Ibanez-Tallon, Ines; Xiao, Cheng; Fitzsimonds, Reiko Maki, et al. The Prototoxin lynx1 Acts on Nicotinic Acetylcholine Receptors to Balance Neuronal Activity and Survival in Vivo. Neuron. 2006; 51(5):587–600. DOI: 10.1016/j.neuron.2006.07.025 [PubMed: 16950157]

Miwa, Julie M.; Walz, Andreas. Enhancement in Motor Learning through Genetic Manipulation of the Lynx1 Gene. PloS One. 2012; 7(11):e43302.doi: 10.1371/journal.pone.0043302 [PubMed: 23139735]

Morishita, Hirofumi; Miwa, Julie M.; Heintz, Nathaniel; Hensch, Takao K. Lynx1, a Cholinergic Brake, Limits Plasticity in Adult Visual Cortex. Science (New York, NY). 2010; 330(6008):1238–40. DOI: 10.1126/science.1195320

Muneoka K, Ogawa T, Kamei K, Muraoka S, Tomiyoshi R, Mimura Y, Kato H, Suzuki MR, Takigawa M. Prenatal Nicotine Exposure Affects the Development of the Central Serotonergic System as Well as the Dopaminergic System in Rat Offspring: Involvement of Route of Drug Administrations. Brain Research Developmental Brain Research. 1997; 102(1):117–26. [PubMed: 9298240]

Nakayama, Hitoshi; Shimoke, Koji; Isosaki, Minoru; Satoh, Hiroyasu; Yoshizumi, Masanori; Ikeuchi, Toshihiko. Subtypes of Neuronal Nicotinic Acetylcholine Receptors Involved in Nicotine-Induced Phosphorylation of Extracellular Signal-Regulated Protein Kinase in PC12h Cells. Neuroscience Letters. 2006; 392(1–2):101–4. DOI: 10.1016/j.neulet.2005.09.003 [PubMed: 16219421]

Nichols, Weston A.; Henderson, Brandon J.; Yu, Caroline; Parker, Rell L.; Richards, Christopher I.; Lester, Henry a; Miwa, Julie M. Lynx1 Shifts α4β2 Nicotinic Receptor Subunit Stoichiometry by Affecting Assembly in the Endoplasmic Reticulum. The Journal of Biological Chemistry. 2014; 289(45):31423–32. DOI: 10.1074/jbc.M114.573667 [PubMed: 25193667]

Parameshwaran, Kodeeswaran; Buabeid, Manal A.; Bhattacharya, Subhrajit; Uthayathas, Subramaniam; Kariharan, Thiruchelvam; Dhanasekaran, Muralikrishnan; Suppiramaniam, Vishnu. Neurobiology of Learning and Memory. Vol. 106. Elsevier Inc; 2013 Nov. Long Term Alterations

in Synaptic Physiology, Expression of β2 Nicotinic Receptors and ERK1/2 Signaling in the Hippocampus of Rats with Prenatal Nicotine Exposure; p. 102-11.

Puddifoot CA, Wu M, Sung RJ, Joiner WJ. Ly6h Regulates Trafficking of Alpha7 Nicotinic Acetylcholine Receptors and Nicotine-Induced Potentiation of Glutamatergic Signaling. Journal of Neuroscience. 2015; 35(8):3420–30. DOI: 10.1523/JNEUROSCI.3630-14.2015 [PubMed: 25716842]

Rogers CA, Gasque P, Piddlesden SJ, Okada N, Holers VM, Morgan BP. Expression and Function of Membrane Regulators of Complement on Rat Astrocytes in Culture. Immunology. 1996; 88(1): 153–61. [PubMed: 8707343]

Schmittgen, Thomas D.; Livak, Kenneth J. Analyzing Real-Time PCR Data by the Comparative CT Method. Nature Protocols. 2008; 3(6):1101–8. DOI: 10.1038/nprot.2008.73 [PubMed: 18546601]

Soni, Neeraj; Kohlmeier, Kristi A. Endocannabinoid CB1 Receptor-Mediated Rises in Ca2+ and Depolarization-Induced Suppression of Inhibition within the Laterodorsal Tegmental Nucleus. Brain Structure and Function. 2015 Jan.doi: 10.1007/s00429-014-0969-4

Srivastava S, Osten P, Vilim FS, Khatri L, Inman G, States B, Daly C, et al. Novel Anchorage of GluR2/3 to the Postsynaptic Density by the AMPA Receptor-Binding Protein ABP. Neuron. 1998; 21(3):581–91. [PubMed: 9768844]

Tanaka M, Marunouchi T, Sawada M. Expression of Ly-6C on Microglia in the Developing and Adult Mouse Brain. Neuroscience Letters. 1997; 239(1):17–20. [PubMed: 9547161]

Tekinay, Ayse B.; Nong, Yi; Miwa, Julie M.; Lieberam, Ivo; Ibanez-Tallon, Ines; Greengard, Paul; Heintz, Nathaniel. A Role for LYNX2 in Anxiety-Related Behavior. Proceedings of the National Academy of Sciences of the United States of America. 2009; 106(11):4477–82. DOI: 10.1073/pnas.0813109106 [PubMed: 19246390]

Thomsen, Morten S.; Arvaniti, Maria; Jensen, Majbrit M.; Lyukmanova, Ekaterina N.; Shulepko, Mikhail A.; Härtig, Wolfgang; Tsetlin, Victor; Mikkelsen, Jens D. Lynx1 Interacts with Multiple Nicotinic Acetylcholine Receptor Subtypes in the Human Brain: Relation to Alzheimer's Disease-like Pathology. Society for Neuroscience Annual Meeting; Washington, DC: 2014.

Thomsen, Morten S.; Cinar, Betül; Jensen, Majbrit M.; Lyukmanova, Ekaterina N.; Shulepko, Mikhail a; Tsetlin, Victor; Klein, Anders Bue; Mikkelsen, Jens D. Expression of the Ly-6 Family Proteins Lynx1 and Ly6H in the Rat Brain Is Compartmentalized, Cell-Type Specific, and Developmentally Regulated. Brain Structure & Function. 2013 Jul.doi: 10.1007/s00429-013-0611-x

Thomsen, Morten S.; Mikkelsen, Jens D. The α7 Nicotinic Acetylcholine Receptor Complex: One, Two or Multiple Drug Targets? Current Drug Targets. 2012; 13(5):707–20. [PubMed: 22300038]

Tsetlin V. Snake Venom Alpha-Neurotoxins and Other 'Three-Finger' Proteins. European Journal of Biochemistry/FEBS. 1999; 264(2):281–86. [PubMed: 10491072]

Wang, H.; Dávila-García, MI.; Yarl, W.; Gondré-Lewis, MC. Neuroscience. Vol. 188. Elsevier Inc; 2011 May. Gestational Nicotine Exposure Regulates Expression of AMPA and NMDA Receptors and Their Signaling Apparatus in Developing and Adult Rat Hippocampus; p. 168-81.

Wang, Hong; Gondré-Lewis, Marjorie C. Prenatal Nicotine and Maternal Deprivation Stress de-Regulate the Development of CA1, CA3, and Dentate Gyrus Neurons in Hippocampus of Infant Rats. PloS One. 2013; 8(6):e65517.doi: 10.1371/journal.pone.0065517 [PubMed: 23785432]

Welsby, Philip J.; Rowan, Michael J.; Anwyl, Roger. Intracellular Mechanisms Underlying the Nicotinic Enhancement of LTP in the Rat Dentate Gyrus. The European Journal of Neuroscience. 2009; 29(1):65–75. DOI: 10.1111/j.1460-9568.2008.06562.x [PubMed: 19077124]

Wu, Meilin; Puddifoot, Clare a; Taylor, Palmer; Joiner, William J. Mechanisms of Inhibition and Potentiation of α4β2 Nicotinic Acetylcholine Receptors by Members of the Ly6 Protein Family. Journal of Biological Chemistry. 2015 jbc M115.647248 doi:10.1074/jbc M115.647248.

Xu W, Orr-Urtreger A, Nigro F, Gelber S, Sutcliffe CB, Armstrong D, Patrick JW, Role LW, Beaudet AL, Biasi M De. Multiorgan Autonomic Dysfunction in Mice Lacking the beta2 and the beta4 Subunits of Neuronal Nicotinic Acetylcholine Receptors. The Journal of Neuroscience: The Official Journal of the Society for Neuroscience. 1999; 19(21):9298–9305. [PubMed: 10531434]

Yu W-F, Guan Z-Z, Nordberg A. Postnatal Upregulation of alpha4 and alpha3 Nicotinic Receptor Subunits in the Brain of alpha7 Nicotinic Receptor-Deficient Mice. Neuroscience. 2007; 146(4): 1618–28. DOI: 10.1016/j.neuroscience.2007.03.002 [PubMed: 17434683]

Zhang, Yifeng; Lang, Qingyu; Li, Jie; Xie, Fang; Wan, Bo; Yu, Long. Identification and Characterization of Human LYPD6, a New Member of the Ly-6 Superfamily. Molecular Biology Reports. 2010; 37(4):2055–62. DOI: 10.1007/s11033-009-9663-7 [PubMed: 19653121]

Zhou, Zhifei; Li, Bei; Dong, Zhiwei; Liu, Fen; Zhang, Yu; Yu, Yang; Shang, Fengqing; Wu, Lizheng; Wang, Xiaojing; Jin, Yan. Nicotine Deteriorates the Osteogenic Differentiation of Periodontal Ligament Stem Cells through α7 Nicotinic Acetylcholine Receptor Regulating Wnt Pathway. PloS One. 2013; 8(12):e83102.doi: 10.1371/journal.pone.0083102 [PubMed: 24376645]

Özhan, Günes; Sezgin, Erdinc; Wehner, Daniel; Pfister, Astrid S.; Kühl, Susanne J.; Kagermeier-Schenk, Birgit; Kühl, Michael; Schwille, Petra; Weidinger, Gilbert. Lypd6 Enhances Wnt/β-Catenin Signaling by Promoting Lrp6 Phosphorylation in Raft Plasma Membrane Domains. Developmental Cell. 2013; 26(4):331–45. DOI: 10.1016/j.devcel.2013.07.020 [PubMed: 23987510]

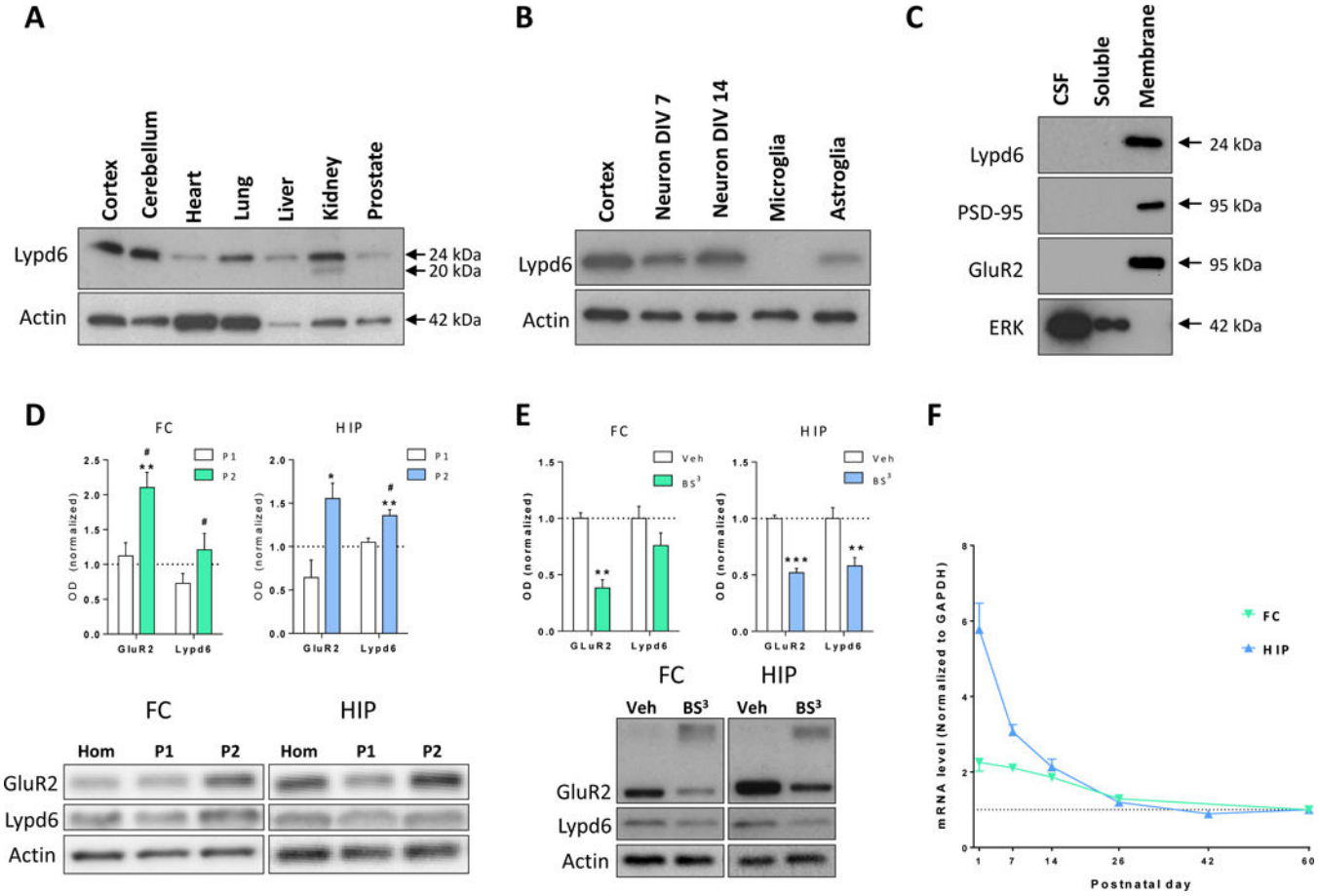

Figure 1. Distribution and developmental expression of Lypd6

(A–E) Representative images and analysis of western blots showing Lypd6 protein levels in: **(A)** different organs of adult male rats (n=2) in relation to Actin, **(B)** cortical tissue from adult male rats, rat cortical primary neurons cultured for 7 or 14 days *in vitro* (Neuron DIV7 and 14, respectively), rat primary microglia cultured for 15 days *in vitro*, and rat primary astroglia cultured for 18 days *in vitro* (n=3) in relation to Actin, **(C)** cerebrospinal fluid (CSF) and soluble and membrane fractions of cortical tissue from adult male rats. The membrane-bound proteins, PSD-95 and GluR2, and the soluble protein extracellular-signal-regulated kinase 1 (ERK) are used as controls for effective fractionation (n=4), **(D)** FC and HIP tissue fractionated using differential centrifugation into a pellet 1 (P1, nuclear) and pellet 2 (P2, crude synaptosome) fraction. Data are normalized to Actin levels and the level of the non-fractionated homogenate (Hom) was set to 1 (dashed line). * $P<0.05$, ** $P<0.01$ indicates statistical difference between non-fractionated homogenate and the P2 fraction, # $P<0.05$ indicates statistical difference between the P1 and P2 fractions in a Bonferroni-corrected ratio paired t-test (n=5), **(E)** minced tissue extracts from the FC or HIP of adult male rats cross-linked with bis(sulfosuccinimidyl) suberate (BS^3) or vehicle (Veh). The staining for GluR2 shows that cross-linking with BS^3 reduces the intensity of the GluR2 band at 95 kDa, and produces a smear of high-molecular weight cross-linked proteins. Data are normalized to Actin levels and the vehicle group was set to 1. ** $P<0.01$, *** $P<0.001$ indicates statistical difference between vehicle- and BS^3-treated tissue in a Bonferroni-

corrected ratio paired t-test (n=9–11). **(F)** Lypd6 mRNA levels in frontal cortex (FC) and hippocampus (HIP) from male rats sacrificed at postnatal day 1, 7, 14, 26, 42, or 60 (n=5–6). The values were normalized to GAPDH levels.

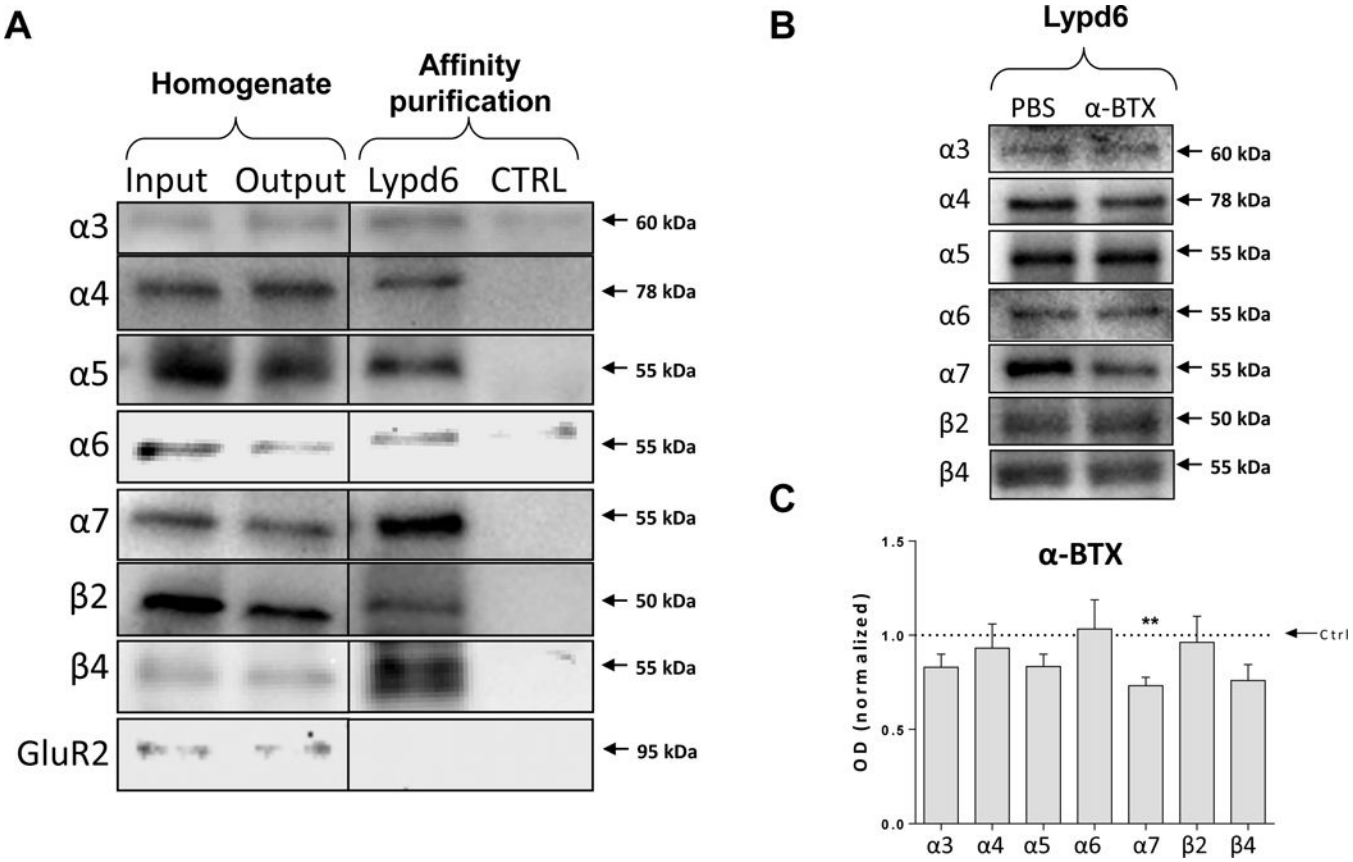

Figure 2. Lypd6 binds multiple nAChR subunits in the human brain

(A) Cortical homogenates from human temporal cortex (Input) were affinity purified using magnetic beads covalently coupled with recombinant human Lypd6 (Lypd6) or non-coupled beads (Ctrl). Also shown is the remaining homogenate after affinity purification (Output). Samples were submitted to gel electrophoresis and western blotting followed by detection of nAChR subunits and the GluR2 AMPA receptor subunit. **(B)** Representative images of western blots of Lypd6 affinity purification of human temporal cortex homogenates pre-incubated with 100 nM α-BTX or vehicle (PBS) for 30 minutes. **(C)** Quantification of data represented in (B), showing that α-BTX interferes with binding of the α7 nAChR subunit to Lypd6-coupled beads (n=5). Values are normalized to their individual vehicle and represented as mean ±SEM. ** $P<0.01$ indicates statistical difference from affinity purification in the absence of α-BTX in a ratio paired t-test.

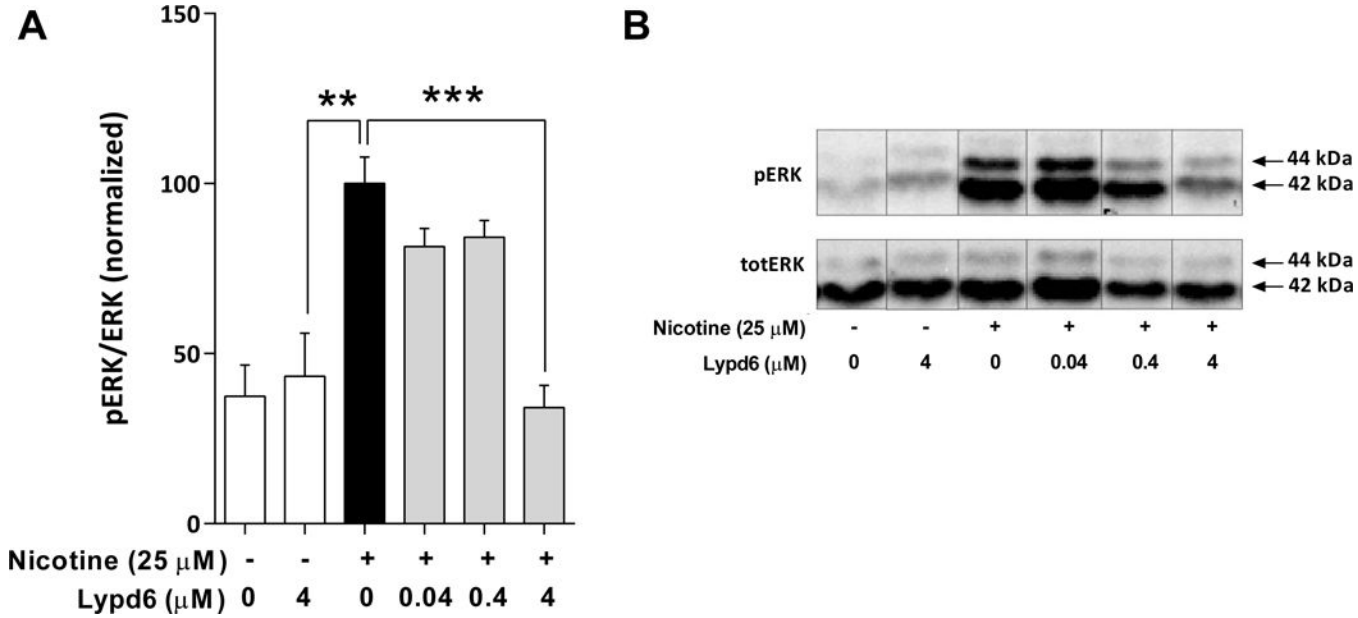

Figure 3. Lypd6 inhibits nicotine-induced ERK phosphorylation

(A) Pre-incubation for 10 minutes with 4 μM recombinant human Lypd6 reduces nicotine-induced ERK phosphorylation in PC12 cells, after stimulation with 25 μM nicotine for 5 minutes. **(B)** Representative images of a western blot membrane summarized in (A), where the phosphorylated isoforms p44 and p42 of the MAP Kinase ERK (ERK1/2) are represented in the top panel (pERK), whereas the total amount of unphosphorylated ERK 1/2 is indicated in the bottom panel (totERK).

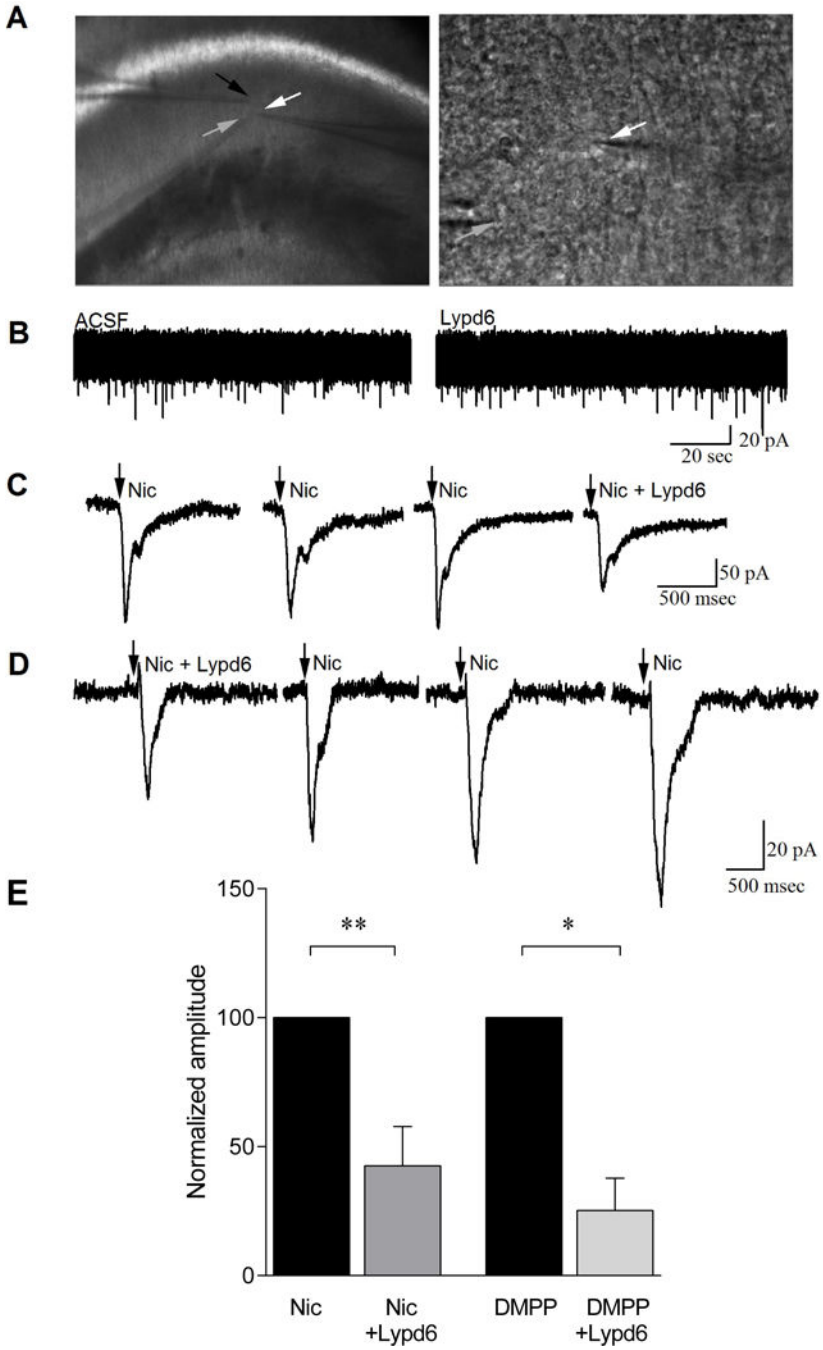

Figure 4. Lypd6 reversibly attenuates nAChR-induced membrane responses in CA1 hippocampal interneurons

(A) Bright field image of the stratum radiatum of the CA1 hippocampal region where recordings were conducted (white arrow indicates recorded cell). Lypd6 (6 μM) was applied via a 2nd patch pipette (black arrow) close to the recorded cell and nicotine was applied via a 3rd pipette (grey arrow). Higher magnification image of a CA1 interneuron recorded for this study (white arrow). The electrode delivering nicotine is also visible (grey arrow). **(B)** Whole-cell, voltage clamp recordings from a CA1 interneuron showing no effect on

induction of inward current by application of Lypd6. **(C)** An example of whole-cell, voltage clamp recordings from a CA1 interneuron showing induction of inward current by application of nicotine (arrow) and attenuation of this current when applied in the presence of Lypd6 (Nic + Lypd6). Nicotine responses were not attenuated with a 3 minute interval between applications, indicating that reductions induced in presence of Lypd6 were not due to cell run down, but were specific to presence of the protein. **(D)** An example of whole-cell voltage clamp recordings from a CA1 interneuron, pre-incubated in Lypd6 for 5 minutes before first application of nicotine, showing that the effect of Lypd6 is lost upon wash-out. The recording examples shown in (C) and (D) are not representing the mean values, but were rather chosen as high-amplitude samples to clearly demonstrate the inhibitory effect of Lypd6. **(E)** Graphs of mean responses to nicotine (n_{cells}=5) and to the non-subtype specific nAChR agonist DMPP (n_{cells}=3) from the population of cells recorded, indicating that when Lypd6 is present, the amplitude of inward currents induced by activation of nAChRs is significantly reduced. Data are displayed as the each cell's response to the agonist in presence of Lypd6 normalized to the same cell's response before the addition of Lypd6. Values are represented as mean ± SEM. * $P < 0.05$, ** $P < 0.01$, indicates statistical difference between groups in a paired t-test.

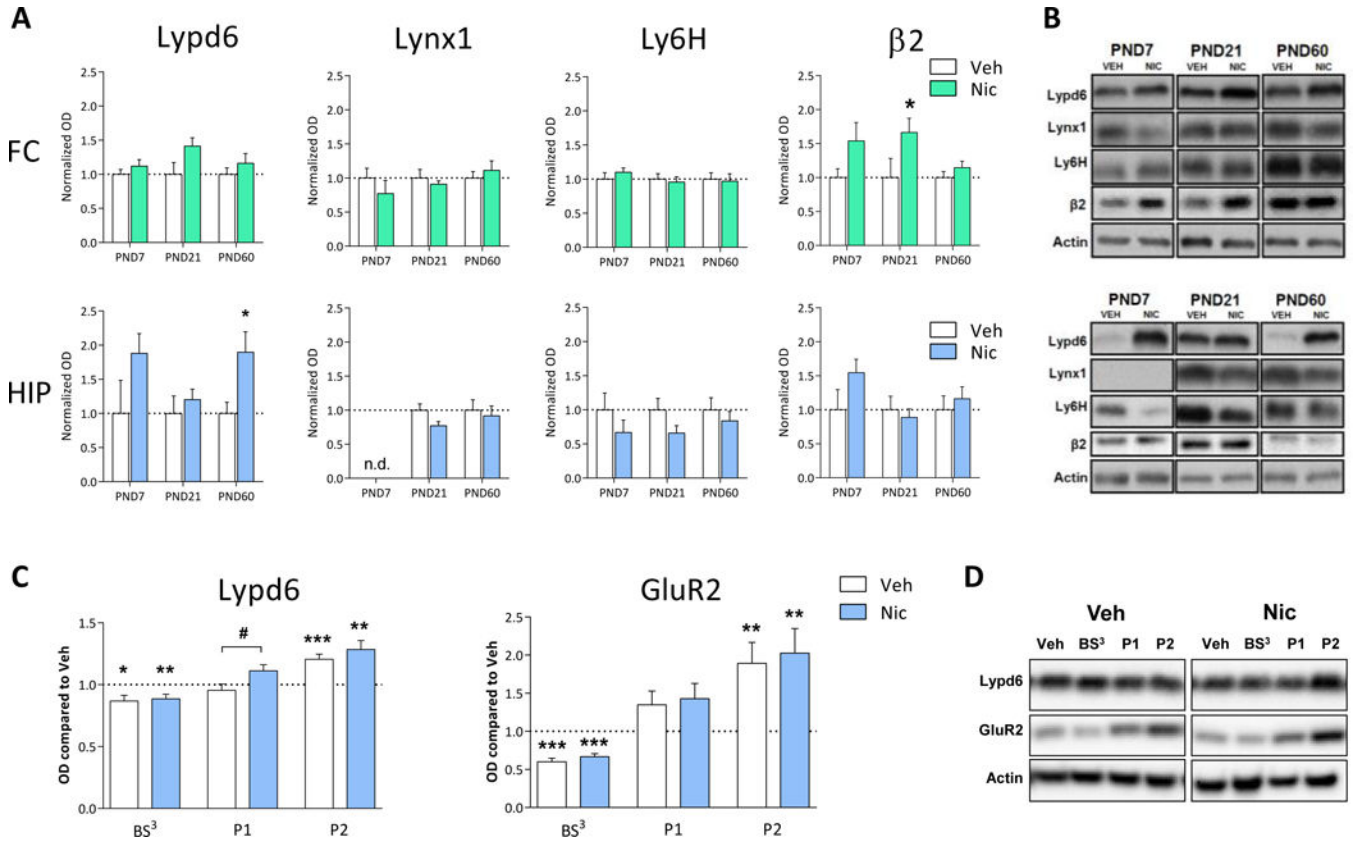

Figure 5. Perinatal nicotine exposure increases hippocampal Lypd6 levels

(A) Quantification of Lypd6, Lynx1 and Ly6H protein levels as well as the β2 nAChR subunit from frontal cortex (FC) and hippocampus (HIP) of male rats exposed to nicotine from embryonic day 7 to postnatal day (PND) 21 through osmotic minipumps implanted into pregnant dams. Animals were euthanized at PND7 (n=5), 21 (n=10) or 60 (n=13). Main effect of nicotine treatment in a two-way ANOVA with age and treatment as the fixed factors is indicated in the graphs. **P*<0.05 indicates statistical difference in a Sidak-corrected multiple comparisons test. **(B)** Representative western blot images of protein levels from FC and HIP at the different ages. **(C)** Quantification of Lypd6 and GluR2 protein levels in hippocampal tissue from the P60 groups described (A), showing that perinatal nicotine exposure increases hippocampal Lypd6 levels in nuclear/endosomal fractions. Tissue was fractionated using differential centrifugation into a pellet 1 (P1, nuclear) and pellet 2 (P2, crude synaptosome) fraction or cross-linked with bis(sulfosuccinimidyl) suberate (BS^3). Data are normalized to Actin levels and the level of the untreated, non-fractionated homogenate was set to 1 (dashed line). * *P*<0.05, ** *P*<0.01, *** *P*<0.001 indicates statistical difference from homogenate in a ratio paired t-test, # *P*<0.05 indicates statistical difference between Vehicle and Nicotine treated groups in an unpaired t-test. **(D)** Representative western blot images of protein levels shown in (C).

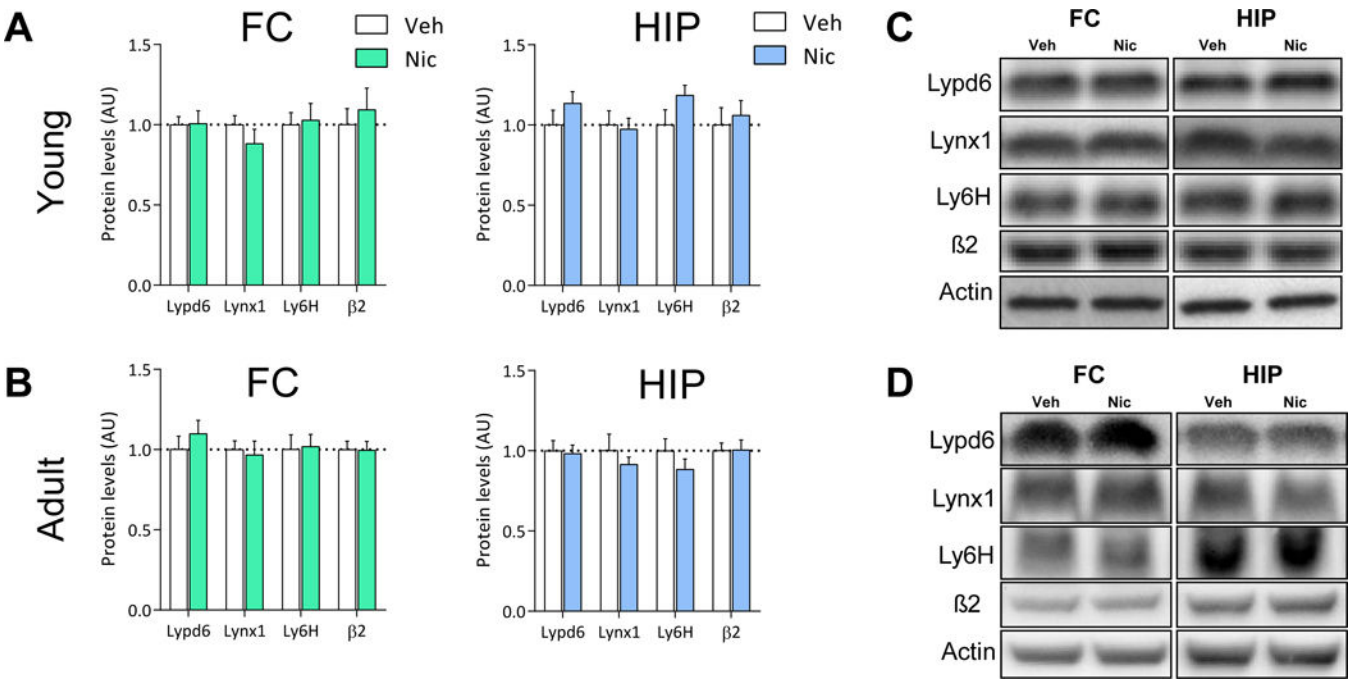

Figure 6. Short-term nicotine exposure does not alter Lypd6, Lynx1 or Ly6H levels in the brain

Lypd6, Lynx1, Ly6H and β2 nAChR subunit protein levels were analyzed in **(A)** frontal cortex (FC) and hippocampal (HIP) tissue from rats administered nicotine (0.4 mg/kg s.c., twice daily) or vehicle (0.9% saline) for 7 days from day 8–14 or **(B)** 54–60 (n=8). **(C and D)** Representative images of western blots summarized in (A) and (B), respectively.

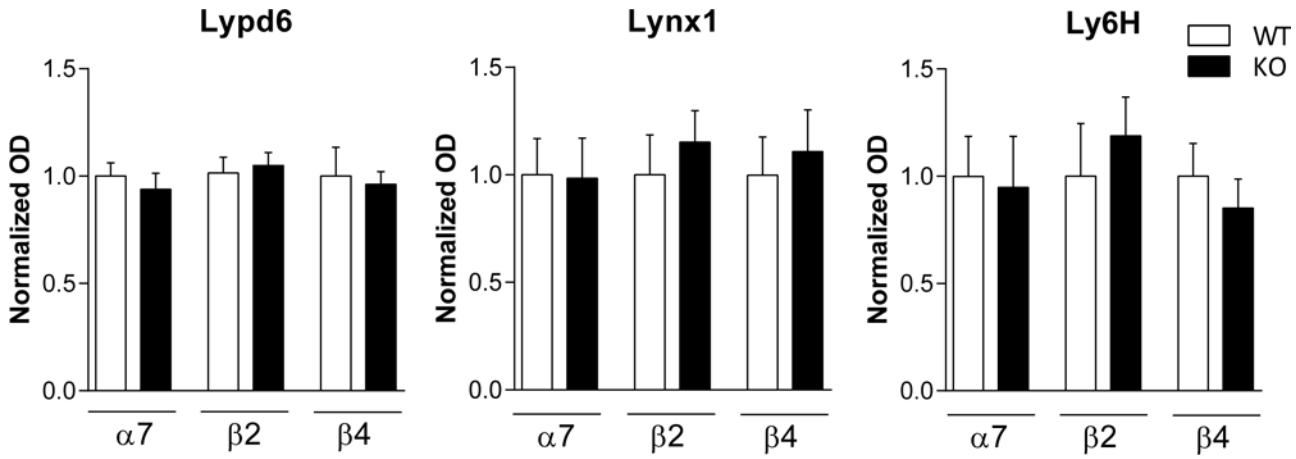

Figure 7. Knock-out of nAChR subunits does not alter Lypd6, Lynx1 or Ly6H levels in frontal cortex

Quantification of Lypd6, Lynx1 and Ly6H protein levels from FC of mice that were either wild-type (WT) or had a genetic deletion (KO) of the β2 (n=7–8), α7 (n=7–8), or β4 (n=4) nAChR subunit gene. Data are normalized to Actin levels and the level of the respective WT was set to 1. Unpaired t-tests revealed no significant differences between WT and KO mice.